# University of Groningen

## Enantiodivergent Sulfoxidation Catalyzed by a Photoswitchable Iron Salen Phosphate Complex

Gilissen, Pieter J.; Chen, Xiaofei; De Graaf, Joep; Tinnemans, Paul; Feringa, Ben L.; Elemans, Johannes A.A.W.; Nolte, Roeland J.M.

**IMPORTANT NOTE: You are advised to consult the publisher's version (publisher's PDF) if you wish to cite from it. Please check the document version below.**

*Document Version*
Publisher's PDF, also known as Version of record

*Publication date:*
2023

[Link to publication in University of Groningen/UMCG research database](#)

# Enantiodivergent Sulfoxidation Catalyzed by a Photoswitchable Iron Salen Phosphate Complex

Pieter J. Gilissen,[+,][a] Xiaofei Chen[+,][a] Joep De Graaf,[a] Paul Tinnemans,[a] Ben L. Feringa,*[b] Johannes A. A. W. Elemans,*[a] and Roeland J. M. Nolte*[a]

*Dedicated to Prof. Takuzo Aida on the occasion of his 65th birthday. We thank him for his seminal contributions to the fields of supramolecular and polymer chemistry.*

**Abstract:** Here we describe a photoswitchable iron(III) salen phosphate catalyst, which is able to catalyze the enantiodivergent oxidation of prochiral aryl alkyl sulfides to chiral aryl alkyl sulfoxides. The stable (S)-axial isomer of the catalyst produced enantioenriched sulfoxides with the (R)-configuration in up to 75% e.e., whereas the photoisomerized metastable (R)-axial isomer of the catalyst favored the formation of (S)-sulfoxides in up to 43% e.e. The maximum Δe.e. value obtained in the enantiodivergent sulfoxidation was 118%, which is identical to the maximum Δe.e. value that was measured in the enantiodivergent epoxidation of alkenes by a related recently described **Mn1** catalyst. This iron-based catalyst broadens the scope of photoswitchable enantiodivergent catalysts and may be used in the future to develop a photoswitchable catalytic system that can write digital information on a polymer chain in the form chiral sulfoxide functions.

## Introduction

The challenging goal of producing both enantiomers of a target molecule (such as a drug) on demand from a single substrate-catalyst combination requires a switching moiety that changes the chirality of the catalyst by means of an external stimulus.[1–3] In this sense, photoswitchable enantiodivergent catalysts are particularly interesting, as light is a facile and non-invasive stimulus.[4,5] Pioneering examples of such catalysts were reported by Feringa and coworkers, who employed light-driven molecular motors for this purpose.[6–10] Axial chirality is a widespread feature in asymmetric catalysts. One of the most versatile building blocks of axially chiral catalysts or ligands is

1,1′-bi-2-naphthol (BINOL). BINOL-phosphoric acids and BINOL-phosphates have been used as chiral inducers in Brønsted acid catalysis[11,12] and in asymmetric counteranion directed catalysis (ACDC).[13,14] Liao and List reported on chiral BINOL-phosphates as chiral inducers of asymmetric epoxidation[15] and sulfoxidation,[16] using manganese(III) salen and iron(III) salen catalysts, respectively.

Work in our group focuses on the encoding of polymer chains with digital information,[17,18] for instance by using chiral epoxides as the digits of the binary code. In order to achieve such an encoding process, we recently designed and synthesized manganese(III) salen phosphate catalyst **Mn1** (Figure 1)[19] and studied its chiroptical and catalytical properties thoroughly. The photoswitchable anionic phosphate ligand changes its axial chirality upon photochemical isomerization between a stable and pseudoenantiomeric metastable isomer, thereby governing dynamic enantioselectivity in catalytic epoxidation reactions. We envisioned that the same catalyst or its iron(III) variant, i.e.,

[a]   Dr. P. J. Gilissen,[+] Dr. X. Chen,[+] J. De Graaf, Dr. P. Tinnemans,
      Dr. J. A. A. W. Elemans, Prof. Dr. R. J. M. Nolte
      Institute for Molecules and Materials
      Radboud University
      Heyendaalseweg 135, 6525 AJ Nijmegen (The Netherlands)
      E-mail: j.elemans@science.ru.nl
              r.nolte@science.ru.nl

[b]   Prof. Dr. B. L. Feringa
      Stratingh Institute for Chemistry
      University of Groningen
      Nijenborgh 4, 9747 AG Groningen (The Netherlands)
      E-mail: b.l.feringa@rug.nl

[+]   These authors contributed equally to this work.

      Supporting information for this article is available on the WWW under
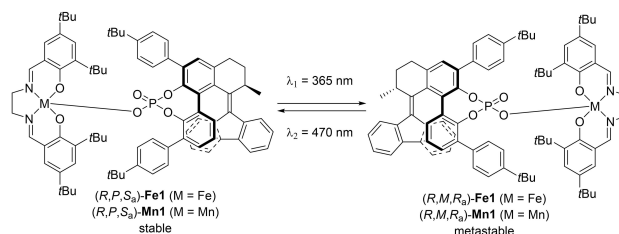      https://doi.org/10.1002/chem.202203539

**Figure 1.** Chemical structures and photochemical isomerization of metal-ligand complexes **Fe1** and **Mn1**. The stereodescriptors of the metal-ligand complexes are the following: central chirality at the stereogenic carbon center, helical chirality around the overcrowded alkene, axial chirality of the bis-aryl motive.

**Fe1** (Figure 1), would also be able to enantioselectively oxidize prochiral sulfides to chiral sulfoxides. The enantiomers of such chiral sulfoxides may also be used as digits of a binary code: (*R*)-sulfoxide = digit 1, (*S*)-sulfoxide = digit 0. Unlike epoxides, sulfoxides have the advantage that they are resistant towards hydrolysis. Furthermore, the oxygen atom of a sulfoxide can readily be removed by means of a proper reducing agent, thereby opening the possibility of "erasing" and "rewriting" a text already written on a polymer chain. A disadvantage of sulfoxides is that they can be further oxidized to achiral sulfones, and in order to avoid such an overoxidation, a chemoselective catalyst is desired. Liao and List previously showed that iron(III) salen catalysts are significantly more chemoselective in sulfoxidation reactions than their manganese(III) analogues.[16] For instance, the reaction of phenyl methyl sulfide (thioanisole) with iodosylbenzene, catalyzed by a manganese(III) salen catalyst equipped with a chiral anionic ligand, gave the corresponding sulfoxide with 50% e.e., and a chemoselectivity (ratio sulfoxide:sulfone) of 2.5:1. In contrast, the iron(III) variant of the same catalyst produced the same sulfoxide with 70% e.e. and a chemoselectivity of 14:1.[16] In this paper we describe the synthesis and enantiodivergent catalytic properties of the new photoswitchable iron salen complex **Fe1**.

## Results and Discussion

**Synthesis and characterization**: The synthesis of complex **Fe1** is depicted in Figure 2, and follows the same strategy as was applied in the synthesis of the related complex **Mn1**. Thus, the achiral iron(III) salen chloride complex **Fe2**[16] was treated with the deprotonated form of racemic or enantiopure phosphoric acid **3**.[19] In order to drive the salt metathesis reaction to completion, **Fe2** was reacted with 1.3 molar equivalents of enantiopure **3** and 1.25 molar equivalents of NaOH in acetone as the solvent. After removal of the solvent and dissolution of the product in dry $CH_2Cl_2$ the formed NaCl was left behind. The presence of a small excess of ligand was considered to be harmless during catalysis.

A single crystal of *Rac*-**Fe1** could be obtained by the slow diffusion of *n*-heptane into a solution of the compound in toluene/chloroform (10:1, v/v). The X-ray crystal structure was found to contain both enantiomers of **Fe1** in the unit cell (Figure 3). Interestingly, in the enantiomer (*R,P,S*$_a$)-**Fe1** (Figure 3A) the iron(III) center adopts a square pyramidal geometry while in the enantiomer (*S,M,R*$_a$)-**Fe1** (Figure 3B) the iron(III)
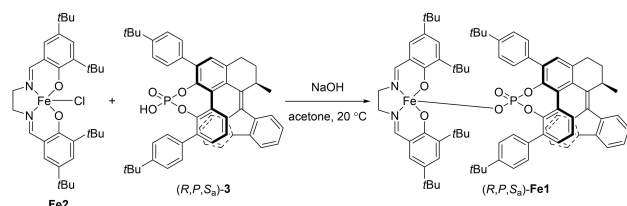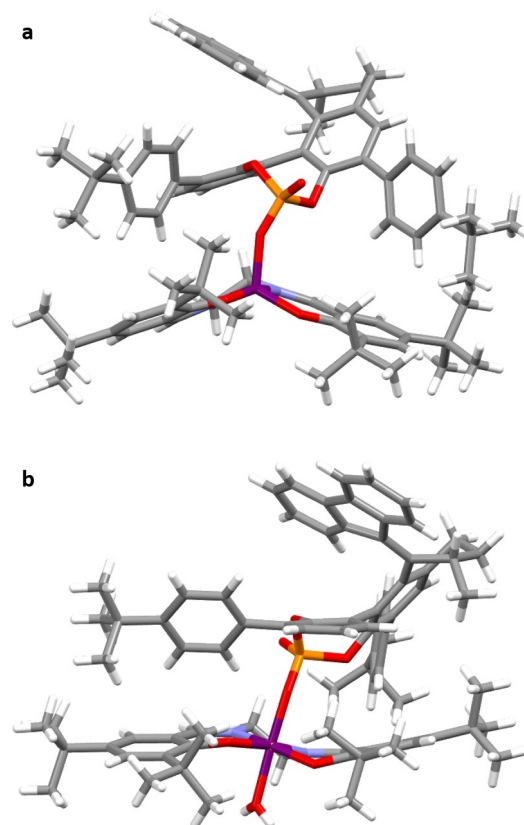


**Figure 3.** X-ray crystal structures of a) (*R,P,S*$_a$)-**Fe1** and b) (*S,M,R*$_a$)-**Fe1**·$H_2O$ found in the unit cell of a single crystal of *Rac*-**Fe1**. Color code: white = hydrogen, grey = carbon, blue = nitrogen, red = oxygen, orange = phosphorus, purple = iron. (Deposition Number 2176423 contains the supplementary crystallographic data for this paper. These data are provided free of charge by the joint Cambridge Crystallographic Data Centre and Fachinformationszentrum Karlsruhe Access Structures service.

center is coordinated to an additional water molecule, forcing it to adopt a distorted octahedral geometry. Although the spatial orientations of the salen moieties are different in the two isomers, the twists in the ethylene diimine bridges are opposite. This feature highlights that regardless of the presence of an additional water ligand, the enantiomers of the phosphate ligand can effectively transfer an opposite chirality to the iron(III) salen moiety.

**Photochemical isomerization**: The photochemical isomerization properties of the phosphoric acid ligand (*R,P,S*$_a$)-**3** and the coordination complex (*R,P,S*$_a$)-**Fe1** were investigated with the help of UV-Vis and ECD spectroscopy (Figure 4a). In our previous report, the photoswitchable features of phosphoric acid **3** were already established in benzene solution, since that solvent gave the best catalysis results in epoxidation reactions.[19] Here, the more environmentally benign solvent ethyl acetate was used for catalysis, as it was found to give identical enantioenrichment as benzene in the sulfoxidation reaction. Therefore, also the photochemical isomerization studies of **3** were carried out in ethyl acetate solution. The forward photochemical isomerization of stable (*R,P,S*$_a$)-**3** to metastable (*R,M,R*$_a$)-**3** was accomplished by UV-irradiation (Fig-
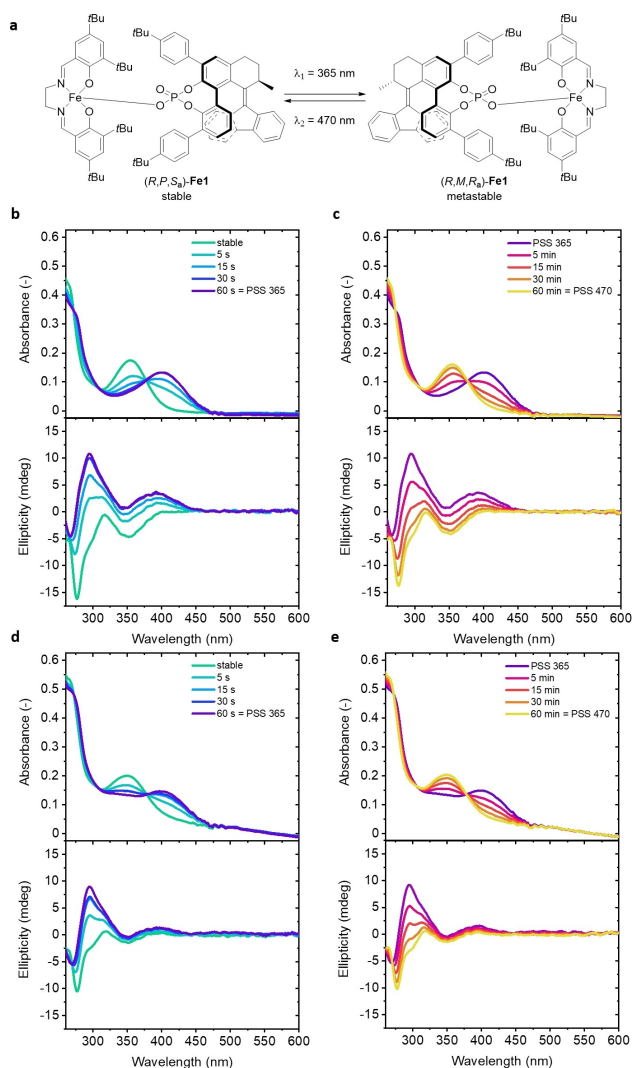


**Figure 2.** Synthesis of iron catalyst (*R,P,S*$_a$)-**Fe1**.

**Chemistry–A European Journal**

Research Article
doi.org/10.1002/chem.202203539

**Chemistry
Europe**
European Chemical
Societies Publishing

**Figure 4.** UV-Vis and ECD spectroscopic studies of the photochemical switching of $(R,P,S_a)$-**3** and $(R,P,S_a)$-**Fe1**.a) Scheme showing the reversible switching of **Fe1**. b) UV-Vis (top) and ECD (bottom) spectra of $(R,P,S_a)$-**3** during switching from the stable to the metastable state upon irradiation with UV light ($\lambda = 365$ nm). c) UV-Vis (top) and ECD (bottom) spectra of $(R,P,S_a)$-**3** during switching from the metastable to the stable state upon irradiation with visible light ($\lambda = 470$ nm). d) UV-Vis (top) and ECD (bottom) spectra of $(R,P,S_a)$-**Fe1** during switching from the stable to the metastable state upon irradiation with UV light ($\lambda = 365$ nm). e) UV-Vis (top) and ECD (bottom) spectra of $(R,P,S_a)$-**Fe1** during switching from the metastable to the stable state upon irradiation with visible light ($\lambda = 470$ nm). For all experiments $c = 5 \times 10^{-5}$ M in EtOAc, $l = 2$ mm, $T = 298$ K.

ure 4b, $\lambda_{max} = 365$ nm). A bathochromic shift of the $\pi \to \pi^*$ transition of the overcrowded alkene moiety from 354 nm to 400 nm was observed ($\Delta\lambda = 46$ nm in ethyl acetate, $\Delta\lambda = 43$ nm in benzene).[19] The presence of a clean isosbestic point at $\lambda = 378$ nm indicated a unimolecular isomerization process. The corresponding ECD spectra revealed that the helicity of the overall molecule inverted, as was evidenced by the inversion of the Cotton effects associated to the $\pi \to \pi^*$ transition, and those centered at $\lambda = 277$ nm (stable isomer) and $\lambda = 295$ nm (metastable isomer). The latter spectral feature could previously not be observed in benzene, as these wavelengths were below the

cut-off wavelength of that solvent. The resulting metastable $(R,M,R_a)$-**3** isomer could be efficiently isomerized back to stable $(R,P,S_a)$-**3** by irradiation with visible light (Figure 4c, $\lambda_{max} = 470$ nm), with retention of the isosbestic point. The photostationary state (PSS) ratios of the forward and backward isomerization process were determined by $^1$H NMR spectroscopy. To this end a sample in ethyl acetate was irradiated to the PSS, the solvent was evaporated, and the residue was redissolved in deuterated benzene enabling the NMR measurement to be performed. Both forward and backward isomerization processes occurred in a near quantitative fashion: PSS$_{365}$ metastable:stable $\approx 94:6$ in ethyl acetate (95:5 in deuterated benzene), and PSS$_{470}$ metastable:stable $\approx 5:95$ in ethyl acetate (5:95 in deuterated benzene).[19]

After having established the photochemical isomerization properties of ligand **3** in ethyl acetate solution, those of the coordination complex **Fe1** were investigated in the same solvent as well (Figure 4d, e). The iron(III) salen moiety showed a very broad absorption band spanning the entire spectrum. Nonetheless, the band corresponding to the $\pi \to \pi^*$ transition of the phosphate ligand could be readily recognized at $\lambda = 350$ nm. When stable $(R,P,S_a)$-**Fe1** was subjected to forward (UV-light) and backward (visible light) photochemical isomerization steps, the spectral changes were very similar to those observed for phosphoric acid $(R,P,S_a)$-**3**. However, the inversion of the Cotton effect associated to the $\pi \to \pi^*$ transition was barely observed, suggesting that the iron(III) salen moiety also shows chiroptical activity at these wavelengths, obscuring the former Cotton effects. Our recent study showed that the phosphate ligand effectively transferred its chirality to the manganese(III) salen moiety of the coordination complex **Mn1**, as was evidenced by the photoswitchable inversion of the Cotton effect at $\lambda = 430$ nm.[19] Surprisingly, the iron(III) analogue **Fe1** did not show such a chiroptical effect (Figure 4d, bottom), possibly because the coordination bond of the phosphate anionic ligand to the iron(III) center is weaker than that to the manganese(III) center. Alternatively, ethyl acetate may be engaged in the process of coordination to the metal center, while benzene presumably would not. The PSS ratios of **Fe1** could not be measured directly with the help of NMR spectroscopy, due to the paramagnetic nature of the compound, but they were assumed to be similar to those of **3**.[19]

**Photoswitchable asymmetric catalysis**: With the optical techniques employed in the previous section it could not be shown with certainty that the axial chirality of the photoswitchable phosphate ligand was transferred to the iron(III) salen moiety of **Fe1**. However, X-ray crystallography clearly evidenced the induction of chirality in the ethylene backbone of the iron(III) salen moiety, and hence it was decided to investigate the enantioselective properties of catalyst $(R,P,S_a)$-**Fe1** and the corresponding pseudoenantiomeric $(R,M,R_a)$-**Fe1** in the sulfoxidation of various prochiral aryl alkyl sulfides (Table 1). We chose ethyl acetate as an environmentally benign solvent for this reaction. The oxidation reaction is hypothesized to proceed through an electrophilic chiral iron(V)oxo intermediate as the reactive species, which is subsequently attacked by the nucleophilic sulfide.[16] When iron(III) catalyst $(R,P,S_a)$-**Fe1** was

*Chem. Eur. J.* **2023**, *29*, e202203539 (3 of 7)

© 2023 The Authors. Chemistry - A European Journal published by Wiley-VCH GmbH

**Table 1.** Enantiodivergent sulfoxidation of aryl alkyl sulfides using **Fe1** as the catalyst.
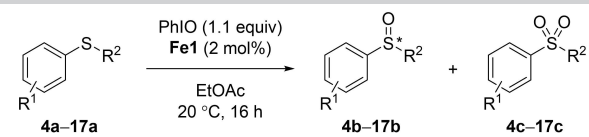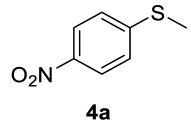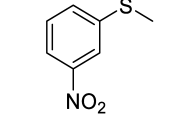


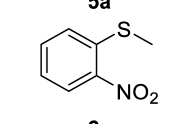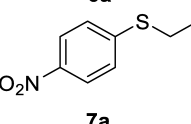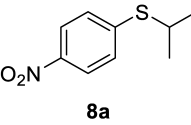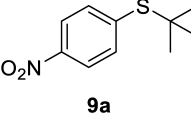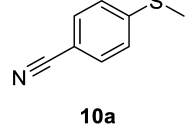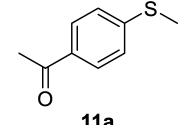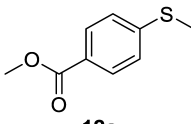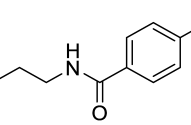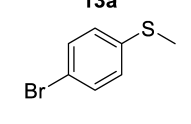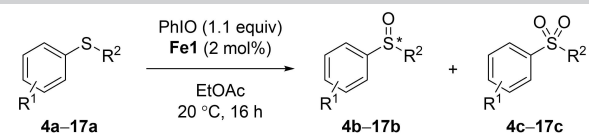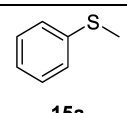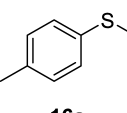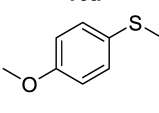| Entry | Substrate | Catalyst | Product ratio[a] a [%] | b [%] | c [%] | e.e. [%][b] | Δe.e. [%] | e.d. [%][c] |
|---|---|---|---|---|---|---|---|---|
| 1 | **4a** | (R,P,Sₐ)-**Fe1** | 27 | 71 | 2 | 64 (R) | | |
| 2[d] | | (R,M,Rₐ)-**Fe1** | 5 | 88 | 7 | 37 (S) | 101 | 58 |
| 3 | **5a** | (R,P,Sₐ)-**Fe1** | 54 | 45 | 1 | 64 (R) | | |
| 4[d] | | (R,M,Rₐ)-**Fe1** | 37 | 62 | 1 | 27 (S) | 91 | 42 |
| 5 | **6a** | (R,P,Sₐ)-**Fe1** | 57 | 43 | 0 | 52 (R) | | |
| 6[d] | | (R,M,Rₐ)-**Fe1** | 51 | 49 | 0 | 17 (S) | 69 | 33 |
| 7 | **7a** | (R,P,Sₐ)-**Fe1** | 25 | 74 | 1 | 71 (R) | | |
| 8[d] | | (R,M,Rₐ)-**Fe1** | 6 | 87 | 7 | 39 (S) | 110 | 55 |
| 9 | **8a** | (R,P,Sₐ)-**Fe1** | 23 | 76 | 2 | 75 (R) | | |
| 10[d] | | (R,M,Rₐ)-**Fe1** | 5 | 90 | 5 | 43 (S) | 118 | 57 |
| 11 | **9a** | (R,P,Sₐ)-**Fe1** | 63 | 36 | 1 | 58 (R) | | |
| 12[d] | | (R,M,Rₐ)-**Fe1** | 69 | 31 | 0 | 27 (S) | 85 | 47 |
| 13 | **10a** | (R,P,Sₐ)-**Fe1** | 16 | 81 | 3 | 65 (R) | | |
| 14[d] | | (R,M,Rₐ)-**Fe1** | 9 | 86 | 5 | 33 (S) | 98 | 51 |
| 15 | **11a** | (R,P,Sₐ)-**Fe1** | 30 | 69 | 1 | 60 (R) | | |
| 16[d] | | (R,M,Rₐ)-**Fe1** | 4 | 88 | 8 | 39 (S) | 99 | 65 |
| 17 | **12a** | (R,P,Sₐ)-**Fe1** | 12 | 85 | 3 | 63 (R) | | |
| 18[d] | | (R,M,Rₐ)-**Fe1** | 11 | 85 | 4 | 41 (S) | 104 | 65 |
| 19 | **13a** | (R,P,Sₐ)-**Fe1** | 5 | 89 | 6 | 52 (R) | | |
| 20[d] | | (R,M,Rₐ)-**Fe1** | 5 | 87 | 8 | 33 (S) | 85 | 63 |
| 21 | **14a** | (R,P,Sₐ)-**Fe1** | 22 | 77 | 1 | 56 (R) | | |
| 22[d] | | (R,M,Rₐ)-**Fe1** | 6 | 89 | 5 | 39 (S) | 95 | 70 |

**Chemistry–A European Journal**

Research Article
doi.org/10.1002/chem.202203539

**Chemistry Europe**
European Chemical
Societies Publishing

**Table 1.** continued



| Entry | Substrate | Catalyst | a [%] | b [%] | c [%] | e.e. [%][b] | Δe.e. [%] | e.d. [%][c] |
|---|---|---|---|---|---|---|---|---|
| | | | | Product ratio[a] | | | | |
| 23 | **15a** | $(R,P,S_a)$-**Fe1** | 7 | 90 | 3 | 51 (R) | | |
| 24[d] | | $(R,M,R_a)$-**Fe1** | 4 | 89 | 7 | 36 (S) | 87 | 71 |
| 25 | **16a** | $(R,P,S_a)$-**Fe1** | 5 | 93 | 2 | 50 (R) | | |
| 26[d] | | $(R,M,R_a)$-**Fe1** | 13 | 83 | 4 | 33 (S) | 83 | 66 |
| 27 | **17a** | $(R,P,S_a)$-**Fe1** | 7 | 89 | 4 | 34 (R) | | |
| 28[d] | | $(R,M,R_a)$-**Fe1** | 4 | 90 | 6 | 27 (S) | 61 | 79 |

[a] Product ratios were determined by comparing the integrals of sulfide/sulfoxide/sulfone protons in the $^1$H NMR spectra of the crude products. [b] Enantiomeric excess values (e.e.) were determined by chiral HPLC, and assignments of the absolute configurations of the enantioenriched sulfoxides were based on optical rotation values (see Supporting Information for details). [c] Enantiodivergence (e.d.) is defined as the ratio of the e.e. values of the enantioenriched sulfoxides when produced by metastable-**Fe1** versus stable-**Fe1**. [d] Catalyst $(R,M,R_a)$-**Fe1** was obtained by irradiation of $(R,P,S_a)$-**Fe1** ($c =$ 1 mg/mL in EtOAc) for 45 min with $\lambda = 365$ nm light, followed by evaporation of the solvent.

used in the oxidation of sulfide **4a** with iodosylbenzene as the oxidant, a 27:71:2 mixture of sulfide **4a**, sulfoxide **4b**, and sulfone **4c** was obtained, showing that **Fe1** displayed satisfactory chemoselectivity (Table 1, entry 1). The enantioenriched sulfoxide (R)-**4b** was obtained with reasonable optical purity (64% e.e.). The pseudoenantiomeric catalyst metastable $(R,M,R_a)$-**Fe1** catalyzed the formation of the opposite enantiomer, i.e., (S)-**4b**, albeit with lower optical purity (Table 1, entry 2, 37% e.e.). This result is in line with the our previous observation that the metastable isomers of the manganese(III) analogue **Mn1** always provided epoxide products with lower enantioenrichment than the stable isomers.[19] This difference may be attributed to two factors.[19] Firstly, the photochemical isomerization is not complete, i.e., the PSS$_{365}$-ratio metastable:stable isomer is not 100:0. Secondly, the phosphorus atom of the phosphate moiety becomes intrinsically chiral once one of its oxygen atoms coordinates to the iron center. If the oxygen-iron bond remains intact during the isomerization process, i.e., the phosphorus atom retains its chirality, the stable and metastable complexes no longer are pseudo-enantiomers, but rather behave as diastereomers and a difference in e.e. is expected. Next, the effect of the position of the nitro substituent of the substrate was investigated (Table 1, entries 3–6). It turned out that the *meta*- and *ortho*-substituted sulfides displayed both lower reactivity and lower enantioselectivity. In a subsequent series of experiments (Table 1, entries 7–12), the effect of the steric bulk of the alkyl substituent at the sulfur atom on the progress and stereoselectivity of the sulfoxidation reaction was monitored. The experiments involving sulfide **7a** (R$^2$ = Et) and **8a** (R$^2$ = iPr) showed nearly identical conversion and enantiose-

lectivities as those involving **4a** (R$^2$ = Me). However, when sulfide **9a** (R$^2$ = tBu) was used, both the conversion and the enantioselectivity dropped significantly. The former observation is attributed to the steric bulk of the *tert*-butyl substituent next to the reactive sulfur atom, making it less accessible for reaction. The drop in enantioselectivity may be explained by the fact that now both the aryl and alkyl substituents of sulfide **9a** are sterically encumbered and hence there is weaker discrimination as to which face of the sulfide will attack the iron(V)oxo intermediate. It has to be noted that the enantioselective sulfoxidation of similar aryl *tert*-butyl sulfides has not been reported before with iron(III) salen catalysts.

In a final set of experiments (Table 1, compare entries 1, 2, 13–28), it was investigated to what extent the electronic properties of the R$^1$-substituent at the *para*-position of the aryl moiety of the sulfide substrate influenced the conversion and enantioselectivity of the sulfoxidation reaction. The substrates are ordered from electron-deficient (R$^1$ = NO$_2$) to electron-rich (R$^1$ = OMe). All substrates showed clean chemoselectivities, with conversions to the sulfoxide ranging from 69% to 93%, regardless of the isomeric state of the used catalyst. Interestingly, the enantioenrichment of the formed sulfoxides was slightly higher for the more electron-deficient sulfides and lower for the more electron-rich sulfides. These results may indicate that the latter, more nucleophilic sulfides have lower barriers for oxidation than the former, less nucleophilic ones, resulting in different (early/late) transition states and therefore less selective reactions with the electrophilic iron(V)oxo intermediate. Liao and List also found that the

more electron-deficient sulfides gave higher enantioselectivities than the more electron-rich ones.[16]

The stable isomer $(R,P,S_a)$-**Fe1** catalyzed the formation of enantioenriched sulfoxides with the $(R)$-configuration (e.e. ranging from 34% to 75%). When instead the corresponding pseudoenantiomeric catalyst $(R,M,R_a)$-**Fe1** was used, $(S)$-sulfoxides were obtained with a lower enantioenrichment (e.e. ranging from 27% to 41%). The difference in e.e. value between the pseudoenantiomeric isomers of catalyst **Fe1** is a measure of the stereoselective performance (maximum obtainable $\Delta$e.e. = 200%). Sulfoxides **4b**–**17b** were obtained with reasonable $\Delta$e.e. values ranging from 61% to 118%. Alternatively, the enantiodivergence (e.d.) of the catalyst may be calculated (maximum obtainable e.d. = 100%).[19] This e.d.-value is a measure of the enantioselective performance of the metastable catalyst with respect to that of the stable catalyst. The sulfoxidation reactions catalyzed by **Fe1** were associated with poor (33%) to good (79%) enantiodivergences.

The enantioenrichment of sulfoxides **4b**,**10b**–**17b** ($R^1$ = variable, $R^2$ = Me) as produced by $(R,P,S_a)$-**Fe1** (red) and $(R,M,R_a)$-**Fe1** (blue) and the associated $\Delta$e.e.-values (black) were plotted as a function of the Hammett para-substituent constant (Figure 5a).[20] It is obvious from Figure 5(a) that sulfides with a more electron-deficient substituent tend to undergo a more enantioselective oxidation with the stable $(R,P,S_a)$-**Fe1** catalyst than sulfides with an electron-rich substituent. In contrast, the metastable $(R,M,R_a)$-**Fe1** catalyst shows a much less significant trend in enantioenrichment as a function of the substituent. In Figure 5(b), the enantiodivergence is plotted versus the Hammett para-substituent constant and the observed correlation is opposite, namely, the e.d.-values decrease from the more electron-rich sulfides to the more electron-deficient sulfides. Initially, it was expected that the enantioselectivity of the pseudoenantiomeric stable and metastable catalysts would show the same relative dependence on the electronic properties of the sulfide substrates, but as the enantiodivergence plot shows this is not the case. A tentative explanation may be that the pseudoenantiomeric stable and metastable phosphate anionic ligands bind with different orientations to the iron(III) center, leading to different degrees of steric interaction between the salen moiety and the sulfide substrate. It is also possible that the substrate approaches the iron(V)oxo intermediate in different ways.

## Conclusion

A photoswitchable iron(III) salen phosphate complex has been prepared and fully characterized by spectroscopic techniques and by an X-ray structure. The complex could efficiently be isomerized with light between two pseudoenantiomeric forms. These isomers were used as catalysts in the enantiodivergent oxidation of prochiral sulfides to chiral sulfoxides. The catalyst stable $(R,P,S_a)$-**Fe1** was able to convert 14 different aryl alkyl sulfides into the corresponding $(R)$-sulfoxides with e.e. values ranging from 34% (electron-rich sulfides) to 75% (electron-deficient sulfides), hence showing a correlation between the
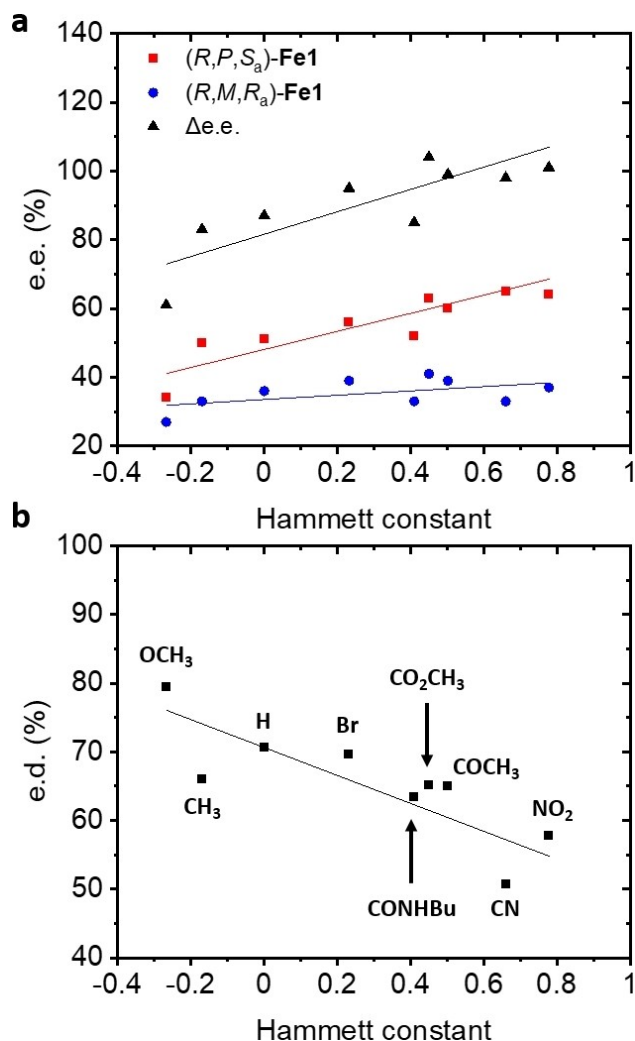


**Figure 5.** Plots displaying a) the enantioselectivities, and b) the enantiodivergences of **Fe1** as a function of the Hammett para-substituent constant. Note that the x-axes in (a) and (b) are identical, and hence the position of the functional groups along the x-axis as indicated in (b) also holds for (a). The linear functions that connect the data points were chosen arbitrarily, just to show the correlation between the e.e.- and e.d.-values and the Hammett para-substituent constant.

electronic properties of the substrate (Hammett para-substituent constant) and the enantioenrichment. The pseudoenantiomer of this catalyst, i.e., metastable $(R,M,R_a)$-**Fe1**, produced enantioenriched $(S)$-sulfoxides with lower enantioselectivities (e.e. between 17% and 43%), and also with a much less pronounced relationship between the Hammett para-substituent constant and the enantioenrichment. The maximum $\Delta$e.e. value obtained in the enantiodivergent sulfoxidation with catalyst **Fe1** was 118%, which is identical to the maximum $\Delta$e.e. value that was measured in the enantiodivergent epoxidation with catalyst **Mn1** as described recently.[19] Hence, it may conclude that the photoswitchable anionic ligand derived from phosphoric acid **3** is an effective and enantiodivergent chiral inducer for both manganese and iron salen complexes. However, further optimization of the ligand structure is required in order to reach higher enantioenrichment

**Chemistry–A European Journal**

Research Article
doi.org/10.1002/chem.202203539

**Chemistry Europe**
European Chemical
Societies Publishing

values. The enantioselective sulfoxidation reaction opens interesting possibilities for the writing of information on polymeric substrates containing sulfide functions in their backbone. Such polymer substrates may be prepared by a polycondensation reaction involving a suitable derivative of ester-containing sulfide substrate **12a** as the monomeric unit.

## Experimental Section

**General procedure for catalysis**: A pre-dried Schlenk finger was charged with racemic or enantiopure catalyst **Fe1** (2.5 mg, 2 mol%). This Schlenk finger was evacuated and backfilled with argon (3×). Then, sulfide substrate **4a**–**17a** (0.10 mmol, 1.0 equiv.) and EtOAc (2.0 mL) were added and the resulting dark red solution was stirred at 20°C for 5 minutes. Subsequently, iodosylbenzene (24.2 mg, 0.11 mmol, 1.1 equiv.) was added in one portion. The resulting mixture was stirred for 16 h in the dark under an argon atmosphere. Thereafter, the solvent was removed in vacuo to afford the crude product. The ratio of sulfide **a** to sulfoxide **b** to sulfone **c** was determined by $^1$H NMR. Then, a pure fraction of the sulfoxide product **b** was isolated using preparative TLC. The pure sulfoxide **b** was subjected to chiral HPLC and optical rotation analysis.

## Acknowledgements

## Conflict of Interest

The authors declare no conflict of interest.

## Data Availability Statement

The data that support the findings of this study are available from the corresponding author upon reasonable request.

[1] J. M. Zimbron, X. Caumes, Y. Li, C. M. Thomas, M. Raynal, L. Bouteiller, *Angew. Chem. Int. Ed.* **2017**, *56*, 14016–14019; *Angew. Chem.* **2017**, *129*, 14204–14207.

[2] S. Kassem, A. T. Lee, D. A. Leigh, V. Marcos, L. I. Palmer, S. Pisano, *Nature* **2017**, *549*, 374–378.

[3] M. Dommaschk, J. Echavarren, D. A. Leigh, V. Marcos, T. A. Singleton, *Angew. Chem. Int. Ed.* **2019**, *58*, 14955–14958; *Angew. Chem.* **2019**, *131*, 15097–15100.

[4] M. Vlatković, B. S. Collins, B. L. Feringa, *Chem. Eur. J.* **2016**, *22*, 17080–17111.

[5] R. Dorel, B. L. Feringa, *Chem. Commun.* **2019**, *55*, 6477–6486.

[6] J. Wang, B. L. Feringa, *Science* **2011**, *331*, 1429–1432.

[7] D. Zhao, T. M. Neubauer, B. L. Feringa, *Nat. Commun.* **2015**, *6*, 6652.

[8] R. Dorel, B. L. Feringa, *Angew. Chem. Int. Ed.* **2020**, *59*, 785–789; *Angew. Chem.* **2020**, *132*, 795–799.

[9] S. F. Pizzolato, P. Štacko, J. C. Kistemaker, T. van Leeuwen, E. Otten, B. L. Feringa, *J. Am. Chem. Soc.* **2018**, *140*, 17278–17289.

[10] S. F. Pizzolato, P. Štacko, J. Kistemaker, T. van Leeuwen, B. L. Feringa, *Nat. Catal.* **2020**, *3*, 488–496.

[11] T. Akiyama, J. Itoh, K. Yokota, K. Fuchibe, *Angew. Chem. Int. Ed.* **2004**, *43*, 1566–1568; *Angew. Chem.* **2004**, *116*, 1592–1594.

[12] D. Uraguchi, M. Terada, *J. Am. Chem. Soc.* **2004**, *126*, 5356–5357.

[13] M. Mahlau, B. List, *Angew. Chem. Int. Ed.* **2013**, *52*, 518–533; *Angew. Chem.* **2013**, *125*, 540–556.

[14] K. Brak, E. N. Jacobsen, *Angew. Chem. Int. Ed.* **2013**, *52*, 534–561; *Angew. Chem.* **2013**, *125*, 558–588.

[15] S. Liao, B. List, *Angew. Chem. Int. Ed.* **2010**, *49*, 628–631; *Angew. Chem.* **2010**, *122*, 638–641.

[16] S. Liao, B. List, *Adv. Synth. Catal.* **2012**, *354*, 2363–2367.

[17] M. G. T. A. Rutten, F. W. Vaandrager, J. A. A. W. Elemans, R. J. M. Nolte, *Nat. Chem. Rev.* **2018**, *2*, 365–381.

[18] J. A. A. W. Elemans, R. J. M. Nolte, *Chem. Commun.* **2019**, *55*, 9590–9605.

[19] X. Chen, P. Gilissen, P. Tinnemans, N. Vanthuyne, F. P. J. T. Rutjes, B. Feringa, J. A. A. W. Elemans, R. J. M. Nolte, *Nat. Synth.* **2022**, 10.1038/s44160-022-00157-7.

[20] L. P. Hammett, *J. Am. Chem. Soc.* **1937**, *59*, 96–103.